A JUVENILE SUBFOSSIL CROCODYLIAN FROM ANJOHIBE CAVE, NORTHWESTERN MADAGASCAR

Joshua C. Mathews[1] and Karen E. Samonds[1]

[1]Department of Biological Sciences
Northern Illinois University
DeKalb, Illinois USA
Email: jmathews4@niu.edu
Ph: 608-290-6247

Keywords: Madagascar; Anjohibe Cave; *Voay robustus*; *Crocodylus niloticus*; Subfossil; Pleistocene; Holocene
pages: 52
pages excluding tables and figures: 40
words (abstract to references inclusive): 10602

Submitted to: *PeerJ*

*Corresponding author

Abstract

Madagascar's subfossil record preserves a diverse community of animals including elephant birds, pygmy hippopotamus, giant lemurs, turtles, crocodiles, bats, rodents, and carnivorans. These fossil accumulations give us a window into the island's past from ~80,000 years ago to a mere few hundred years ago, recording the extinction of some groups and the persistence of others. The crocodylian subfossil record is limited to two taxa, *Voay robustus* and *Crocodylus niloticus*, found at sites distributed throughout the island. *V. robustus* is extinct while *C. niloticus* is still found on the island today, but whether these two species overlapped temporally, or if *Voay* was driven to extinction by competing with *Crocodylus* remains unknown. While their size and presumed behavior was similar to each other, nearly nothing is known about the growth and development of *Voay*, as the overwhelming majority of fossil specimens represent mature adult individuals.

Here we describe a nearly complete juvenile crocodylian specimen from Anjohibe Cave, northwestern Madagascar. The specimen is referred to *Crocodylus* based on the presence of caviconchal recesses on the medial wall of the maxillae, and to *C. niloticus* based on the presence of an oval shaped internal choana, lack of rostral ornamentation and a long narrow snout. However, as there are currently no described juvenile specimens of *Voay robustus*, it is important to recognize that some of the defining characteristics of that genus may have changed through ontogeny. Elements include a nearly complete skull and many postcranial elements (cervical, thoracic, sacral, and caudal vertebrae, pectoral elements, pelvic elements, forelimb and hindlimb elements, osteoderms). *Crocodylus niloticus* currently

inhabits Madagascar but is locally extinct from this particular region; radiometric dating indicates an age of ~460 – 310 years before present (BP). This specimen clearly represents a juvenile based on the extremely small size and open sutures/detached neural arches; total body length is estimated to be ~1.1m (modern adults of this species range from ~4 – 6 m). This fossil represents the only juvenile subfossil crocodylian specimen reported from Madagascar.

Introduction

The island country of Madagascar is considered a hot spot for biodiversity due to its high level of endemism (Myers et al., 2000). While the island is currently under intense study by scientists researching the extant fauna, many questions still remain about when and how this fauna arrived (e.g., Samonds et al., 2013). Madagascar has been isolated in the Indian Ocean for over 80 million years and most of the fauna is thought to have arrived on the island during this time (Storey et al., 1995; Ali & Huber 2010; Samonds et al, 2012).

Crocodylomorpha has a long evolutionary history dating back to the Late Triassic, ~230 mya (Irmis et al., 2013; Zanno et al., 2015), and have had a largely global distribution for most of their evolutionary history. The earliest known crocodylomorph fossils on Madagascar date back to the early Jurassic with the teleosaurid *Steneosaurus baroni* Newton 1893. However the Late Cretaceous Maevarano Formation in the Mahajanga Basin (Buckley et al., 2000; Buckley, 2001)

90 preserves a very diverse assemblage of notosuchian, mahajangasuchid, and
91 trematochampsid crocodylomorphs that includes *Simosuchus clarki* Buckley et al.,
92 2000, *Mahajangasuchus insignis* Buckley & Brochu, 1999, *Araripesuchus*
93 *tsangatsangana* Turner, 2002, and *Miadanasuchus oblita* (Buffetaut & Taquet, 1979),
94 (Buckley et al., 2000; Buckley, 2001; Krause et al., 2006; Rasmusson Simons &
95 Buckley, 2009; Turner, 2006; Turner & Sertich, 2010). While this Cretaceous
96 assemblage is unique in its diversity, these groups of crocodylomorphs became
97 globally extinct following the end Cretaceous mass extinction event (O'Connor et al.
98 2010).
99 In contrast to this Cretaceous assemblage, the Cenozoic fossil record of
100 Madagascar is relatively unknown largely due to the lack of terrestrial deposits.
101 Because of this, little is known about crocodylians from this time period. Today, the
102 only living Malagasy crocodylian is the Nile crocodile, *Crocodylus niloticus* Laurenti,
103 1768 (Brochu, 2007), which has also been reported from subfossil assemblages (e.g.,
104 Bickelmann & Klein, 2009). The only other subfossil crocodylian reported from
105 Madagascar is *Voay robustus* Grandidier & Vaillant, 1872, an extinct form from the
106 Late Pleistocene and Holocene (Brochu, 2007).
107 Many subfossil sites (subfossil referring to the relatively young age and
108 incomplete mineralization of the remains) across the island have produced
109 crocodylian remains (Brochu, 2007; Muldoon et al. 2012; Goodman & Jungers, 2014,
110 Rosenburger et al., 2015). However, due to the extensive interest in the origins of
111 the elephant birds, lemurs and other mammals, subfossil crocodylians have been
112 largely overshadowed. The near lack of Cenozoic fossils, and the recognition of only

two crocodylian taxa in the subfossil record, *Voay robustus* and *Crocodylus niloticus*, has led to questions regarding whether they ever coexisted (Brochu, 2007; Bickelmann & Klein, 2009); some have suggested the recent form (*Crocodylus*) outcompeted *Voay* (Burney et al., 1997). Owing to the fact that very little is known about either of these genera on the island, a better understanding of their paleobiology is needed to more rigorously test this hypothesis.

In 2003, an expedition to Anjohibe Cave in northwest Madagascar (Fig. 1) recovered the disarticulated remains of a small crocodylian from one small puddle within the cave system. The remains include a nearly complete skull and mandible, a nearly complete cervical series, most of the thoracic vertebrae, one sacral vertebra, one caudal vertebra, elements of the forelimb and hind limbs, elements of the pectoral and pelvic girdle, ribs, numerous osteoderms, and many isolated teeth (Fig. 2, 3 & 4). Radiometric dating has indicated that the specimen dates to ~460 – 310 years BP (Crowley & Samonds, 2013).

The specimen described here, UAP-03.791, is a young individual due to the presence of open sutures and/or detached neural arches of the vertebral column. However, since all known specimens of *V. robustus* are from adult individuals, and we know virtually nothing of its growth and development, it is difficult to eliminate the possibility that the specimen could represent *Voay*. Both *C. niloticus* and *V. robustus* have been reported from Anjohibe Cave (Goodman & Jungers, 2014). While some postcranial elements of *Voay* differ from extant crocodylians (Brochu, 2007), these elements have not been recovered or are too incomplete to distinguish. In order to assign a proper diagnosis, we compare here the new juvenile specimen to

136 those of young and adult *C. niloticus* and adult *V. robustus*, and use additional
137 methods (e.g., CT scanning) to incorporate details of the growth and development of
138 *Crocodylus* into our analysis.

139 **Geological Setting**

140 Anjohibe Cave is located in northwestern Madagascar, northeast of
141 Mahajanga (Fig. 1), and is found on the southern part of the current dry savannah of
142 the Mahavo plains (Samonds, 2007). It is part of a large karst system that is formed
143 within the Eocene limestone plateau with many kilometers of passages and over
144 two dozen entrances (Burney et al. 1997; Samonds, 2007). Anjohibe has been
145 extensively studied for decades and has provided us with some of the best evidence
146 documenting environmental change in and around the cave over the last 40,000
147 years (Brook et al. 1999; Burney et al. 1997, Goodman & Jungers, 2014). Thousands
148 of fossils have been collected from Anjohibe Cave; these include a diverse and very
149 well preserved fauna including numerous species of birds, crocodiles, turtles, bats,
150 rodents, tenrecs, hippos, carnivorans, the aardvark-like *Plesiorycteropus* and 11
151 species of lemur (e.g., MacPhee, 1994; Burney et al. 1997; Godfrey & Jungers, 2002;
152 Samonds, 2007; Faure et al. 2010).

153

154 **Institutional Abbreviations**

155 FMNH – Field Museum of Natural History, Chicago, Illinois, United States of America
156 UAP- Université d' Antananarivo Paléontologie, Antananarivo, Madagascar
157 UCMP – University of California Museum of Paleontology - Berkeley, California,
158 United States of America

Systematic Paleontology

Eusuchia Huxley 1873

Crocodylia Gmelin 1789, sensu Benton & Clark 1988

Crocodylidae Cuvier 1807

Crocodylus niloticus Laurenti 1768

Materials and Methods

Both dry and wet specimens of young *Crocodylus niloticus* were examined from collections at the University of California Museum of Paleontology, Berkeley, California and from the Amphibians & Reptiles collection at the Field Museum of Natural History, Chicago, Illinois. Both articulated and disarticulated skulls were examined so as to understand and identify disarticulated elements of the Malagasy specimen and how they might articulate with one another. Additionally, skulls from adult specimens of *C. niloticus* and *V. robustus* were examined from collections at the Université d' Antananarivo Paléontologie in Antananarivo, Madagascar.

Because of the limited number of available skulls of young individuals, one wet specimen of *C. niloticus* was scanned using computed tomography (CT) to better visualize the internal anatomy. CT was performed with a Toshiba Aquilion 64 multislice CT scanner with 64 detector channels (Toshiba America Medical Systems, Inc., Tustin, CA) at Rockford Memorial Hospital, Rockford, Illinois, USA. Scanning thickness was prescribed at 0.50 mm with 0.25 mm overlapped image reconstruction. Image matrix was 512 x 512 x 16. The scanned volume data set was

transferred to a computer workstation where volume rendered multiplanar and 3D images were created with Vitrea Software (Vital Images, Inc., Minnetonka, MN).

Description

Skull

The right premaxilla is nearly complete preserving five alveoli (Fig. 3). It forms the anterior and lateral margin of the external naris and articulates posteromedially with a small anterior process of the nasal bones. A posterior process projects backward where it articulates laterally with the right maxilla. Of the alveoli, the second premaxillary alveolus, pm 2, is the smallest whereas pm 4 is the largest. Pm 1 appears to project nearly directly out of the front of the snout (procumbent) whereas the remaining alveoli appear to project ventrolaterally. There is no foramen for the lower dentary tooth present on the premaxilla. The left premaxilla was not recovered.

The right maxilla is nearly complete and preserves 11 alveoli with what appears to be a broken 12th (Fig. 3C). The maxilla narrows at the maxillary tooth 4, m 4, alveolus where the notch for the dentary tooth 4, is present. The m 5 alveolus is the largest in the tooth row and is circular in shape. Posteriorly the alveoli become smaller and more oval in shape. One tooth remains in the m 9 alveolus. Occlusion pits are present between the alveoli for acceptance of the lower tooth row. As with most crocodylians, the dorsal surface bears a sculptured texture. Medially, the caviconchal wall of the maxilla is well preserved and bears a linear series of shallow recesses (Fig. 5).

The left maxilla is less complete, however it does preserve a nearly complete length, missing only its articular surface with the premaxilla and sutural contact with the ectopterygoid (Fig. 3C). The external wall of nearly all of the alveoli are broken and missing, however the presence of at least 10 alveoli can be confirmed. The alveolus for m 5 is the largest in the tooth row. Occlusion pits are not preserved. As with the right maxilla, a linear series of shallow recesses are present on the medial caviconchal wall.

The nasal bones are long and slightly convex laterally and contribute over two-thirds to the length of the snout (3A). A V-shaped anterior process extends forward where they articulate with the premaxillae posterior to the external naris, widening posteriorly along their length, narrowing where they unite with the lacrimal, prefrontal and frontal. The nasals contact the maxillae along an underlapping suture along its length, and makes up the dorsal surface of the nasal passage.

Both left and right jugals are preserved and nearly complete (Fig. 3A). They form the lateral margin of the orbit and the ventral margin of the infratemporal fenestra. Anteriorly and anteroventrally they contact the maxilla along an overlapping suture. The anterior ramus of the jugal unites with the maxilla above the last four to five alveoli in the maxillary tooth row. The anterior ramus of the jugal further contacts the lacrimal dorsomedially. Medially, an ascending process rises from the center of the jugal forming the ventrolateral half of the postorbital bar. The postorbital bar forms the posterior margin of the orbit and the anterior margin of the infratemporal fenestra. The posterior ramus of the jugal forms the

ventral border of the infratemporal fenestra and unites with the quadratojugal posterodorsally. The jugals are widest along their middle at the postorbital bar, and taper along their anterior and posterior rami.

Both lacrimals are preserved. The left lacrimal is missing roughly half of the anterior portion while the right is nearly complete (Fig. 3A). They are roughly half as wide as they are long and form the anterior margin of the orbit. They contact the jugal laterally, pre-frontals medially and the maxilla anteriorly. Along the margin of the orbit near the contact with the prefrontal, the lacrimal thickens. Along the anterior margin of the orbit, within the prefrontal-lacrimal suture lies the lacrimal duct foramen.

The prefrontals are triangular in shape with their length approximately twice their width (Fig. 3A). Medially the prefrontals contact the posterior process of the nasals and the anterior process of the frontal. Anterolaterally the prefrontals contact the lacrimals along a slightly concave suture due to a ridge at the orbit. They form the anteromedial margin of the orbit where they are thickened. The prefrontal pillars extend ventrally, and are relatively uniform in length. Midway along the length of the pillars a small process extends medially where it unites with the corresponding pillar forming an opening through which the olfactory tract runs.

The frontal bone sends an anterior process forward between the two prefrontal bones uniting with the posterior process of the nasals (Fig. 3A). The lateral margins of the frontal are thickened and form the medial border of the orbit. The sutural contact with the postorbitals and the parietal are sinuous and fairly distinct as compared with the other cranial sutures owing to its juvenile stage. The

ventral surface bears a deep U-shaped trough running anteroposteriorly roofing the olfactory tract. Posteriorly the ridges of this trough terminate as two protuberances where they articulate with the laterosphenoids.

The postorbital is roughly kidney-shaped along its dorsal surface and contacts five cranial elements (Fig. 3A). A postorbital process descends ventrally where it contacts the ascending process of the jugal forming the dorsal half of the postorbital bar. The medial suture of the postorbital contacts the frontal along its anterior half and the parietal along its posterior half. The postorbital unites with the squamosal posteriorly on the lateral side of the main body along an overlapping suture. Ventrally it contacts the laterosphenoid immediately medial to the postorbital bar. The posterior margin of the postorbital forms the anterior border and one half of the lateral border of the supratemporal fenestra.

The parietal lies posterior to the frontal and forms the middle portion of the skull table, roofing the braincase (Fig. 3A). It is laterally expanded anteriorly where it unites with the frontal along its anterior margin and with the postorbitals laterally. The parietal constricts posteriorly forming an interfenestral bar that is flat dorsally and forms the medial walls of the supratemporal fenestrae. The dorsal surface of the interfenestral bar is narrow expanding ventrally, constricting the supratemporal fenestral opening. Posteriorly the parietal expands again articulating with the squamosals laterally and the supraoccipital on its posteroventral margin. A small V-shaped wedge of the supraoccipital is present on the dorsal surface of the skull table. Ventrally the parietal articulates with the laterosphenoids anteriorly and the quadrates posteriorly along the wall of the braincase.

The squamosal forms the posterolateral corner of the skull table and the posterolateral margin of the supratemporal fenestra (Fig. 3A & 3B). The posteriormost corners are upturned to form what appear to be incipient horns or "hornlets." The structures are very small and seem to be covered with mineral deposits or possible preserved connective tissue, giving them the appearance of horns. The squamosal contacts the postorbital anteriorly along an underlapping suture that extends forward to the postorbital bar. Medially, the squamosal contacts the parietal behind the supratemporal fenestra and dorsal to the temporal canal. While it lies very close to the supraoccipital, the squamosal does not make contact with it, instead forming the dorsal margin of the posttemporal fenestra. The squamosal is expanded laterally and posterolaterally where it forms the dorsal roof and part of the posterior wall of the external otic aperture. Ventrally the squamosal articulates with the quadrate anteriorly below the squamosal/postorbital suture and posterolaterally a squamosal process unites with the ramus of the quadrate. The same squamosal process unites with the paroccipital process of the exoccipital posteroventrally. The lateral surface of the squamosal bears a groove that houses musculature for the earflap.

One nearly complete right quadratojugal is preserved and bridges the space between the jugal and the quadrate at the posterolateral corners of the skull (Fig. 3B). Anteriorly it articulates with the posterior ramus of the jugal. Posteriorly it articulates with the ramus of the quadrate where it forms half of the posterior margin of the infratemporal fenestra. A small process extends anteriorly into the infratemporal space, however this is broken. The quadratojugal extends posteriorly

296 nearly the entire length of the ramus of the quadrate however it terminates just
297 prior to the distal end and has no contribution to the mandibular condyle of the
298 quadrate.

299 Two completely preserved quadrates were recovered from the specimen.
300 The quadrate forms both the posterolateral wall of the brain case and the floor and
301 partial posterior margin of the external otic aperture (Fig. 3A-C). Anterior to the otic
302 aperture lies the preotic foramen. Anterior to the preotic foramen a thin lamina
303 forms the posterodorsal half of the posterior margin of the infratemporal fenestra.
304 Dorsally, the quadrate articulates with the laterosphenoids, squamosal, and the
305 parietal forming one half of the ventral wall of the supratemporal fenestra. Ventrally
306 the quadrate expands forming the posterior and ventral margin of the trigeminal
307 foramen, however both quadrates are damaged in this region and only a small
308 portion of the posterior margin of the trigeminal foramen can be seen on the right
309 quadrate. Ventral to the trigeminal foramen the quadrate articulates with the
310 pterygoid and the basisphenoid. The ramus of the quadrate extends posteriorly
311 articulating with the quadratojugal laterally and with the paroccipital process of the
312 exoccipital medially before forming the mandibular condyle that articulates with the
313 mandible.

314 The palatines, though incomplete, are long and narrow extending posteriorly
315 from their articular surface with the maxilla at the level of tooth position 7 to unite
316 with the pterygoids at the end of the tooth row (Fig. 3C). They form the lateral walls
317 and floor of the nasal cavity and the medial border of the suborbital fenestrae.
318 Anteriorly they expand laterally where they contact the maxilla and posteriorly

where they contact the pterygoids. The left palatine preserves a small dorsal process that articulates with the prefrontal pillar; the right process is broken.

Both ectopterygoids were recovered and are nearly complete, missing only a small portion of the anterior maxillary process and small portions of the descending rami (Fig. 3C). The anterior process of the ectopterygoid articulates laterally with the maxilla throughout most of its length, running medial to the posterior maxillary tooth row and forming the lateral margin of the suborbital fenestra. The right ectopterygoid extends to the border of the tenth and eleventh maxillary alveoli. Although it is incomplete, the sutural surface on the maxilla ends at the middle of m 10 indicating that only the very tip of the anterior process is missing. The anterior process of the left ectopterygoid extends to about the same distance and similarly is missing only the anterior-most tip. The ascending process of the ectopterygoid articulates with the jugal and forms the lateral half of the lower half of the postorbital bar. The descending ramus of the ectopterygoid articulates posteroventrally with the pterygoid buttress and the main body of the pterygoid along an underlapping suture. As with the anterior processes, the descending rami are also missing their distal tips.

The pterygoid is the ventral-most part of the basicranium and forms the roof of the nasopharyngeal duct dorsal to the palatines (Fig. 3C). The juvenile pterygoids are incomplete, preserving the main body and pterygoid buttress. The anterior process is broken and only represented by fragments; in complete specimens the posterior portion of the pterygoids completely enclose the duct behind the suborbital fenestrae before exiting at the internal choanae. The anterior process

splits, forming a septum with separate chambers that are floored by the paired palatines. The anterior process extends to the anterior margin of the suborbital fenestra. Posteriorly the pterygoid expands laterally forming wings that are dorsoventrally thickened and form a buttress at the articular surface with the ectopterygoid. Near the midline, dorsal to the internal choana, a thin lamina extends dorsally on each side forming a V-shaped saddle where the basisphenoid sits. Two posterior pterygoid flanges are located immediately posterior to the internal choana and ventral to the median eustachian foramen. The ascending lamina forming the saddle for the basisphenoid articulates laterally with the quadrate.

Both laterosphenoids are partially preserved. The laterosphenoids enclose the anterior portion of the braincase and meet at the midline. Anteriorly they contact the main body of the frontal dorsally where they form the ventral opening for the olfactory tract. Ventral to the olfactory opening they form the opening for the optic nerve. They articulate posteroventrally with the basisphenoid before contacting the quadrate forming the anterior border of the trigeminal foramen. Dorsally they contact the postorbital and parietal.

The supraoccipital lies on the dorsal midline of the occipital region (Fig. 3A). It is a heart-shaped element wedged between the exoccipitals above the foramen magnum and posteroventral to the parietal (Fig. 3D). A small V-shaped wedge is present on the dorsal surface of the skull roof. The lateral surface forms a protuberance on each side that is an attachment site for epaxial muscles. These protuberances further form the ventral border of the posttemporal fenestra through which occipital veins pass.

The exoccipitals are well preserved; they form the lateral walls and roof of the foramen magnum (Fig. 3D). Laterally they expand forming the paroccipital processes that articulate with the posterior ramus of the quadrates. The exoccipitals come together at the midline forming a small condyle immediately dorsal to the foramen magnum. Dorsally they articulate with the supraoccipital. Several foramina can be seen lateral to the occipital condyle. A small foramen punctures the lateral wall of the foramen magnum through which runs cranial nerve XII. Immediately lateral to cranial nerve XII is a larger foramen housing the vagus nerve. Ventral to the vagus foramen is the lateral carotid foramen.

A partially preserved basisphenoid was recovered. The basisphenoid nests between the dorsal processes of the pterygoids and forms the anterolateral walls and anterior floor of the braincase. It articulates dorsally with the laterosphenoids and posteriorly with the quadrate. Anteriorly a cultriform process extends forward over the body of the pterygoids, however it is broken and missing in this specimen. The posterior surface is broken; the median eustachian foramen is preserved ventral to the basioccipital tubera.

The basioccipital is well preserved in the specimen (Fig 3D). The most prominent feature is the occipital condyle, which articulates with the vertebral column and forms the floor of the foramen magnum. Laterally it articulates with the exoccipital. Ventrally it bears a prominent dorsoventral ridge immediately below the occipital condyle with shallow fossae on each side. The basioccipital articulates anteroventrally with the basisphenoid and sits snugly in a V-shaped saddle of the basisphenoid. Anteriorly the dorsal surface of the basioccipital forms the floor of the

posterior portion of the braincase. On the articular surface with the basisphenoid a small channel forms the medial wall of the lateral eustachian opening. Ventral to the occipital condyle an indentation is present that forms the roof of the median eustachian opening. The lateral eustachian openings lie at approximately the same level of the median eustachian opening, as is typical in *Crocodylus* (Brochu, 2000).

Mandible

The dentary makes up the anterior two thirds of the length of the mandible (Fig. 6). Eleven complete alveoli are preserved in the right dentary with what appears to be three more in the posterior of the tooth row. The left dentary is less complete than the right preserving eight whole and four and a half partial alveoli. The anterior-most portion of the dentary is missing. However, because the fourth alveolus is the largest in the tooth row, and preserved on this specimen with two in front, only the anterior-most alveolus is missing on each side. The mandibular symphysis is nearly complete and extends posteriorly to the posterior border of the fourth alveolus. Posteriorly the dentary expands dorsoventrally where it contacts the surangular dorsally forming about one half of the dorsal margin of the external mandibular fenestra. Posteroventrally it articulates with the angular and contributes to one half of the ventral margin of the fenestra, however only a small portion is preserved. The Meckelian groove is preserved and runs along the medial dentary posterior to the symphysis expanding posteriorly.

Both splenials are incompletely preserved. The right is more complete, missing a small portion of the anterior and posterior ends. The left is fragmentary and represented only by a long sliver of the ventral margin and a smaller section of

411 the dorsal margin. The splenial in crocodylids is a thin flat bone forming the medial
412 wall of the mandible and Meckelian groove. It thickens on its posterodorsal margin
413 where it forms the medial wall of the posterior tooth row. It articulates with the
414 dentary laterally and the angular, surangular, and coronoid posteriorly, although
415 only a small portion of the articular surface with the angular and surangular is
416 preserved on both preserved elements.
417 The surangular forms the dorsal portion of the posterior end of the mandible
418 and contributes one-third to the length (Fig. 6). Anteriorly it forms the
419 posterodorsal margin of the external mandibular fenestra and contacts the dentary
420 along an overlapping sutural contact where the dentary slots in medially. A medial
421 process extends forward medially behind the dentary and bears an articular surface
422 for the splenial. Posteriorly, the surangular articulates medially with the articular
423 and forms the lateral wall of the glenoid fossa. Ventrally it contacts the angular
424 behind the external mandibular fenestra along an underlapping suture.
425 The angular forms the ventral portion of the posterior end of the mandible
426 and contributes about one half of the total length (Fig. 6). Anteriorly it unites with
427 the dentary sending an elongate process ventral to the dentary and wrapping
428 around to the medial side where it articulates with the splenial forming the floor of
429 the Meckelian groove. Laterally it forms the ventral border and one half of the
430 posterior border of the external mandibular fenestra. Posteriorly the angular
431 ascends dorsally where it laterally overlaps the lower half of the articular and
432 retroarticular process.

The articular is a small bone at the posterior-most end of the mandible and forms the articular joint with the skull (Fig. 6). The anterodorsal surface of the articular bears the glenoid fossa. The glenoid fossa is the articular surface for the quadrate. It is slightly constricted medially and flares laterally where it contacts the surangular. Two depressions are present on the surface of the glenoid where the mandibular condyles of the quadrate articulate and though they are of equal depth, the medial side is narrower than the lateral. Posterior to the glenoid fossa, the articular hooks posterodorsally with a concave surface forming the retroarticular process, which serves as the attachment for the *m. depressor mandibulae*. On the medial surface of the articular where the retroarticular process meets the glenoid is the foramen aereum. A small lingual foramen is located on the anterior surface of the articular ventral to the lateral fossa of the glenoid. Medial and ventral to the articular process is a deep trough for attachment of the *m. pterygoideus dorsalis*.

The coronoid is a small mediolaterally compressed bone of the lower jaw forming the posterior and ventral margin of the mandibular fossa and anterior margin of the medial intermandibular foramen. The left coronoid is complete whereas the right coronoid is missing a large portion of the anteroventral process as well as a small posteriorly directed process.

Teeth

Only one tooth was found preserved in situ on the right maxilla. Thirty-eight teeth were found at the site in association with the remains. Nineteen of these had full or partially preserved roots, while the remaining 19 teeth were crowns only. Most of them are conical shaped with a weakly striated lingual surface and carinae

on the anterior and posterior margin (Fig. 7). A few teeth from the posterior toothrow were recovered and are shorter and more bulbous than the conical anterior teeth (Fig. 7).

Vertebral Column

Most crocodylians have a vertebral formula of eight or nine cervical vertebrae, ten thoracic vertebrae, five lumbar vertebrae, two sacral vertebrae and about 30 – 40 caudal vertebrae (Griggs & Kirshner, 2015). The specimen described here preserves 23 complete or partial vertebrae (Fig. 2). Seven cervical vertebrae are preserved including a nearly complete atlas and a complete axis, 13 thoracic or lumbar vertebrae, one sacral vertebra, one sacral rib and one caudal vertebra. At least four anterior thoracic vertebrae can be positively identified by the presence of a keeled centrum and a hypapophysis on the anterior ventral surface. Mid to posterior thoracic vertebrae do not maintain these features and without the transverse processes cannot be distinguished from lumbar vertebrae. All of the recovered vertebrae are procoelous.

The atlas (C1) is not fused into one solid element like the rest of the vertebrae (Fig. 8A). It is made up of a dorsal proatlas, an intercentrum and paired neural arches (only the left lateral neural arch was recovered). The intercentrum is wedge-shaped with a concave dorsal surface and prominent diapophyses on the ventrolateral surface where the atlantal ribs articulate. The left neural arch rests above the intercentrum and forms the lateral wall of the neural canal. Ventrally it is robust with an articular facet on the anterior surface where it meets the occipital condyle of the skull. A second articular facet is present on the posterior surface

where the arch contacts the odontoid process of the axis. The neural arch narrows dorsally before expanding anteroposteriorly and arching medially where it articulates with the proatlas on its anterior dorsal surface. The proatlas is a boomerang V-shaped bone forming the roof of the neural canal. It points anteriorly with the lateral "wings" terminating in articular facets where they contact the neural arches.

A complete axis (C2) with unfused odontoid process was recovered (Fig. 8B). The neural arch is attached to the centrum, however it is not completely fused; there is an open neurocentral suture. The centrum has a prominent ventral keel with a bifurcated hypapophysis anteriorly. The anterior sutural surface of the centrum is crenulated where it articulates with the corresponding surface of the odontoid process. Posteriorly the centrum forms a ball joint where it articulates with the adjacent vertebra. The neural arch is shallow dorsoventrally and possesses a short neural spine that runs the length of the vertebra. The prezygapophyses are small and weakly developed and positioned dorsolaterally where they articulate with the neural arch of the atlas. The postzygapophyses are larger and more developed, overhanging the neural canal at the posterior end of the neural spine. They are positioned ventrolaterally where they articulate with the prezygapophyses of the next vertebra. The odontoid process of the axis is disarticulated from the centrum. It is "petal" shaped with two articular facets on each side where the axial rib attaches. A short and stout process projects anteriorly from the anterodorsal surface.

There are five remaining cervical vertebrae preserved. Four are complete to nearly complete whereas one is a partial neural arch. They are similar in

morphology to one another with minor differences. They are procoelous and have cylindrical shaped centra with a pronounced hypapophysis on the anterior part of the ventral surface (Fig. 8C). Lateral to the hypapophysis is a capitular facet that receives the capitulum of the cervical rib head. The neural arch is dorsoventrally expanded and bears a long and thin posteriorly projecting neural spine. Anterior to the neural spine, the paired prezygapophyses project forward with medially inclined articular surfaces. Posterior to the neural spine are the paired postzygapophyses that project posteriorly with ventrolateral articular surfaces. Along the anterior sutural surface with the centrum lies a small weakly developed ventrolaterally directed transverse process that receives the tuberculum of the cervical rib head. Proceeding posteriorly in the cervical series, the hypapophysis, capitular facets, transverse processes, and zygapophyses become more pronounced as the vertebrae increase in size and the ribs become larger.

Thirteen vertebrae representing the thoracic and lumbar region of the specimen are preserved. In crocodylians, thoracic and lumbar vertebrae are very similar in size and shape and are often indistinguishable from each other without the preserved transverse processes and diapophyses. The first four thoracic vertebrae can be identified by the presence of a well-developed hypapophysis on the anterior ventral surface of T1, decreasing in size to small and weakly developed on T4 (Fig. 8E). The remaining thoracic vertebrae lack a hypapophysis. As with the cervical series, all of the thoracic and lumbar vertebrae are procoelous with spindle shaped centra. T1 has a very pronounced hypapophysis that hooks forward. The capitular facet has migrated dorsally on the vertebra, however it is still borne on the

centrum at the level of the neurocentral suture. The presence of the capitular facet on each side gives the anterior condyle an oval shape. The neural arch is dorsoventrally expanded, however not to the extent seen in the cervical vertebrae. The neural spine is incomplete; however the base is sufficiently preserved to show that it is still quite thin. The prezygapophyses still maintain their dorsomedial articular surfaces although they are becoming more dorsally directed. Likewise, the postzygapophyses still maintain their ventrolateral articular surface; however they are becoming more ventrally directed. The transverse process is more developed than those in the cervical series and become more laterally projecting. They are not large however, and are rod-like in shape and located about half way up the neural arch.

Moving posteriorly in the vertebral column, the capitular facet continues to migrate dorsally spanning the neurocentral suture in T2 after which it is entirely born on the neural arch in the later vertebrae. The transverse process continues this pattern migrating dorsally where it begins near the top of the neural arch, just ventral to the neural spine in T2 and thereafter. The transverse process of T2 still maintains a rod-like shape, but the process is expanded anteroposteriorly in T4 and flattens out in the following vertebrae. As the capitular facet is now located on the neural arch, the centra become more circular in shape throughout the remainder of the vertebral column.

The remaining nine thoracic and lumbar vertebrae include two nearly complete vertebrae, three centra with partial neural arches, one complete centrum, one partial centrum, and two partial neural arches (Fig. 2 & 8D). None of them have

548 preserved transverse processes so it is difficult to assign them to a specific region;
549 based on size and shape, the majority seem to be from the thoracic region.
550 There are only two sacral vertebrae in crocodylians (Griggs & Kirshner,
551 2015). One nearly complete sacral vertebra (S1) and one partial sacral rib (S2) are
552 preserved (Fig. 8F). Sacral vertebrae are different from the rest of the vertebral
553 column in that they do not exhibit procoelous centra. The first sacral vertebra is
554 concave anteriorly, as in all other vertebrae, however the posterior articular surface
555 is flat. Likewise, the second sacral vertebra has a flat anterior articular surface and a
556 concave posterior articular surface. The preserved specimen exhibits the concave
557 anterior surface and flat posterior surface, which identifies it as S1. The centrum is
558 wider than it is high and has an oval shape. The neural arch is relatively shallow
559 dorsoventrally and lacks a preserved neural spine. The neural canal is smaller in
560 size giving the neural arch a more heavily robust form. The prezygapophyses and
561 postzygapophyses are well developed. The sacral ribs contact the vertebrae along a
562 broad suture that spans half of the centrum and half of the neural arch. A partial
563 right sacral rib is present on the specimen however the left sacral rib is missing. A
564 partial sacral rib was recovered in the deposit that does not articulate with S1,
565 suggesting it likely belongs to S2. The rib is too incomplete to determine which side
566 of the vertebra it belongs.
567 One caudal vertebra has been identified from the site. It consists of a nearly
568 complete centrum with a partial neural arch. The centrum is long and thin and
569 spindle-shaped with typical procoelous form. The preserved neural arch is a thin
570 lamina of the left lateral wall of the neural canal. A small broken surface of a

transverse process is present on the neural arch. The shape, size, and presence of a transverse process suggest it is an anterior to mid-caudal vertebra. There is no visible sign of a neurocentral suture present on the vertebra, which is consistent with previous reports of juvenile crocodylians (Brochu, 1996; Ikejiri, 2012).

Forelimb & Pectoral Girdle

The right scapula is incomplete, preserving most of the proximal end including the glenoid and articular surface with the coracoid and about one third of the scapular blade (Fig. 4C). The deltoid crest, while incomplete, is slender and located on the anterodorsal surface of the scapular body. The scapular blade narrows immediately behind the scapular body before expanding distally.

The left coracoid is nearly complete, missing only a small wedge from the distal blade and a small portion of the articular surface for the scapula (Fig. 4B). The coracoid is a flat bone with expanded proximal and distal ends. The body is pierced by the coracoid foramen anterior to the glenoid. The coracoid blade expands distally where it articulates with the sternum.

A partial left humerus was recovered from the site representing approximately two thirds of the proximal end (Fig. 4A). The humeral head is thin, but well developed. The deltopectoral crest is well developed though gracile.

Few elements from the manus were recovered. Those that were, include both the left and right radialae and one metacarpal (Fig. 4D-F). The left radiale is complete whereas the right one is missing a small portion of the distal articular surface. The complete metacarpal is wider at its proximal end and has a slight twist distally.

Hindlimb & Pelvic Girdle

The left ilium is fragmented and preserves the dorsal margin of the acetabulum and a portion of the posterior process (Fig. 4G). The supra-acetabular crest is thickened and rugose on its anterodorsal surface and becomes a small ridge as it passes posteroventally. The posterior process is incomplete and is thin and blade-like where preserved.

An element tentatively referred to as the left ischium preserves the proximal and mid-shaft to just prior to its distal expansion (Fig. 4H). Most of the acetabulum is missing with only a small portion of the middle section preserved.

The left pubis, while damaged, preserves most of its length missing only the distal end (Fig. 4I). Half of the proximal articular surface of the pubis is preserved. The pubic shaft narrows briefly before expanding toward the distal end, which is eroded.

What appears to be the left tibia is preserved as a nearly complete half (Fig. 4J). The epiphyses of the proximal and distal ends are not preserved, however the remaining length of the shaft is. Most of the entire one half of its length is missing or severely damaged. Due to the damage, this identification is tentative.

A possible left fibula was also recovered. It is nearly complete, missing only the distal articular surface (Fig. 4K). The proximal end is moderately expanded narrowing distally before expanding laterally at the distal end where it has been damaged. The proximal surface is semi-circular in cross-section. Although damaged, it appears that the distal surface exhibits the same semi-circular cross-section.

Some elements from the pes were recovered. Although exact identification of each element is difficult, three metatarsals, five pedal phalanges, and the left calcaneus were collected (Fig. 4L-O). Two of the three metatarsals are complete and have been assigned to the right pes. The remaining metatarsal has been designated as from the left pes and is nearly complete, missing the distal condyle and a small section of the shaft. Four of the pedal phalanges are complete while one phalanx is nearly complete and missing only a small portion of the proximal articular surface. Three of the phalanges appear to be from the right pes, while the remaining two are from the left.

Discussion

Assessing Maturity

Brochu (1996) documented that neurocentral suture closure in crocodylians progresses in a caudal to cranial direction. Most of the neurocentral sutures in the caudal vertebrae of *Alligator mississippiensis* Daudin, 1802, were closed or partially closed in all hatchlings whereas the neurocentral sutures in all presacral and sacral vertebrae were completely open. The odontoid process-axis centrum suture closes prior to the neurocentral suture in *A. mississippiensis* and *Crocodylus acutus* (Brochu, 1996). Additionally the sacral ribs remain separate from the vertebral body. This pattern of suture closure was consistent with other crocodylians including *C. acutus* Cuvier, 1807, *Osteolaemus tetraspis* Cope, 1861, and *Alligator sinensis* Fauvel, 1879 (Brochu, 1996). Using histological methods, Ikejiri (2012) further investigated neurocentral suture closure by examining the cartilaginous layers between the

neural arch and the centrum, the synchondroses, through ontogeny in *A. mississippiensis*. This work corroborated the caudal to cranial pattern of neurocentral suture closure initially described by Brochu (1996). Interestingly, Ikejiri (2012) found that this pattern was reversed in the sacral vertebrae, with the anterior sacral fusing prior to the posterior sacral. While exploring allometric trends through ontogeny, Ikejiri (2015) also documented negative allometry in the diameter of the neural canal in *A. mississippiensis*. Hatchling specimens maintain a neural opening that is proportionally large relative to the centrum and vertebral height, whereas the neural canal in adult specimens is proportionally much smaller (Ikejiri, 2015). The specimen described here exhibits a complete lack of suture closure in all of the presacral and sacral vertebrae, most of which have completely detached neural arches (Fig. 8). The odontoid process is completely detached from the axis centrum. Only one caudal vertebra was recovered and there is no neurocentral suture visible. In all of the recovered vertebrae with complete or partial neural arches, the neural canal is large relative to the centrum and vertebral height. Although the neural canal is not as large as that seen in a hatchling, its size is consistent with what could be expected in a juvenile individual.

The degree of fusion or lack thereof exhibited by fossil skulls has often been used to characterize the growth stage of the animal. Numerous studies of non-avian dinosaurs have used fusion of the skull as a proxy for skeletal maturity (Sampson et al., 1997; Longrich & Field, 2012; Bailleul et al., 2016). While this has become a relatively common practice, Bailleul et al. (2016) found that this is not the case in crocodylians. Their study documented the sequence and timing of cranial fusion of

skulls of the emu, *Dromaius novaehollandiae* Latham, 1790, and *A. mississippiensis* through ontogeny. While the pattern of cranial fusion in *D. novaehollandiae* follows an expected pattern of open sutures in young individuals becoming progressively closed as the animal matures, the inverse is found to occur in *A. mississippiensis*. As the alligator grows, the cranial sutures become wider, never allowing the elements to fuse together. While it is uncertain why this occurs, Bailleul et al. (2016) suggest that it may be attributed to species-specific biomechanics as the animal preys upon larger food sources. Although the skull of the described specimen was found in complete disarticulation and has been subsequently reassembled, it cannot be referred to a juvenile status based on this alone.

Systematic Placement

The overall shape and morphology of the subfossil skull bears a strong resemblance to a juvenile *C. niloticus* (Fig. 9). UCMP 140795 and UCMP 140796 represent young *C. niloticus* ~3.5 years of age. Other than a slight size difference these specimens appear to be nearly identical to the subfossil skull. It should be noted, however that snout shape is known to vary within crocodylian species and should not be used to make taxonomic judgment (Brochu, 2007). Additionally, because no known juvenile specimens of *V. robustus* are known, taxonomic placement based on shape alone should be avoided.

The shape of the internal choana is a character used to distinguish between *C. niloticus* and *V. robustus* (Brochu, 2007). The internal choana of *V. robustus* has a distinct circular shape where it exits the pterygoids and has a pronounced choanal neck (Fig. 10). This characteristic is also seen in the extant species *Osteolaemus*

685 *tetraspis* and *O. osborni* and is a distinct synapomorphy placing *Voay* within the
686 Osteolaeminae (Brochu, 2007). The internal choana of *C. niloticus* on the other hand
687 is oval in shape (Fig. 10) and lacks the distinct choanal neck that is seen in *V.*
688 *robustus*. As illustrated in figure 10, the subfossil specimen exhibits the oval shape
689 choana morphology suggesting it belongs to *C. niloticus*. Further evidence
690 supporting this placement is FMNH 37216; a juvenile *C. niloticus* (Fig. 10) as well as
691 those of UCMP 140795 and UCMP 140796. The internal choanae of these specimens
692 are nearly identical to that of the subfossil specimen. It could be argued that this
693 character could change through ontogeny in *Voay*, however Brochu (2007) noted
694 that this condition is consistent throughout ontogeny in *Osteolaemus*. An
695 examination of a growth series of skulls of *Crocodylus acutus*, with which *C. niloticus*
696 share a close phylogenetic relationship, shows that the observed oval/D-shaped
697 internal choana in this taxon does not change through ontogeny.
698 A second character that further supports the placement of the subfossil
699 specimen within *C. niloticus* is the presence of well-developed caviconchal recesses
700 on the medial wall of the maxilla. Both maxillae recovered in the subfossil specimen
701 preserve a linear series of pockets projecting into the medial caviconchal wall (Fig.
702 5). In most crocodylians, the medial wall of the caviconchal recess is smooth,
703 whereas extant *Crocodylus* possess the described pockets (Witmer, 1995; Brochu,
704 2000; Brochu, 2007). These recesses are not present in the maxilla of *V. robustus*
705 and are a derived feature of the crown genus *Crocodylus* (Brochu, 2007). Because
706 these cavities are absent from maxillae of *V. robustus* and *Osteolaemus*, and they are
707 a derived feature of *Crocodylus*, it seems that this character lends unequivocal

support toward referring the specimen to *C. niloticus*.

One of the most prominent characteristics of *V. robustus* is the large squamosal horn on the posterolateral corner of the squamosal (Fig. 11). Squamosal horns are not uncommon among crocodylians and are present in extinct and extant taxa. In addition to *V. robustus*, extinct forms include *Crocodylus anthropophagus* Brochu et al., 2010, and *Aldabrachampsus dilophus* Brochu, 2006, while extant forms include *Crocodylus rhombifer* Cuvier, 1807, *Crocodylus siamensis* Schneider, 1801, and *C. niloticus* (Brochu, 2000; Brochu et al., 2010). Very old *Crocodylus porosus* have been documented having a very distinctly concave cranial table, suggesting the presence of squamosal horns (Mook, 1921a). Although squamosal horns can be observed in some adult *C. niloticus*, they are less prominent than they are in *Voay* and may be absent altogether. The Cuban crocodile, *C. rhombifer* and the Siamese crocodile, *C. siamensis* have demonstrated that squamosal horns vary through ontogeny (Delfino & De Vos, 2010). While mature adults are characterized by well-developed squamosal horns, juveniles' horns are underdeveloped or absent (Brazaitis, 1973; Brochu, 2010; Delfino & De Vos, 2010). The subfossil specimen does appear to possess very small, yet distinct squamosal growths or "hornlets". The horns appear to have a mineral deposit or preserved connective tissue on them which could give them a more pronounced appearance. While the CT image of the modern juvenile *C. niloticus* (FMNH 37216) lacks even the smallest amount of growth on the posterolateral corners of the squamosals, it should be noted that this specimen is very young and UCMP 140795, UCMP 140796 and UCMP 123091 all show squamosal "hornlets" similar to those seen in the subfossil specimen (Fig. 12).

731 Because squamosal horns are not found exclusively in *V. robustus* and are known to
732 show ontogentic variation (Brazaitis, 1973; Delfino & De Vos, 2010), their presence
733 on the subfossil appear to be inconsequential.

734 The lack of discrete preorbital crests or rostral bosses distinguishes the
735 specimen from inclusion within New World or Indopacific *Crocodylus* (Brochu,
736 2000; Brochu et al., 2010). In New World crocodiles such as *C. rhombifer* or
737 *Crocodylus moreletii* A.H.A. Duméril & Bibron, 1851, elevated nasals impart a boss
738 extending from the anterior lacrimals forward to the posterior premaxillae (Brochu,
739 2000). Likewise, Indopacific crocodiles, including *C. porosus* Schneider, 1802, and *C.*
740 *siamensis* possess preorbital ridges on the dorsal surface of the snout (Mook, 1921b;
741 Brochu, 2000). These features are not found on *C. niloticus* nor are they found on the
742 preserved rostral bones of this specimen.

743 **Cryptic Species**

744 Until recently, there were thought to be only three species of crocodylians
745 known throughout Africa and Madagascar (Schmitz et al., 2003): *Mecistops*
746 *cataphractus* Cuvier, 1807, *Osteolaemus tetraspis*, and *Crocodylus niloticus*. The Nile
747 crocodile, *C. niloticus,* was thought to be widespread across most of Africa and
748 Madagascar (Schmitz et al., 2003). A surge of molecular studies over the last decade
749 or so has aimed to elucidate relationships within Crocodylia in attempts to separate
750 subspecies or to seek out potential cryptic species within established crocodylian
751 populations (Ray et al., 2001; Schmitz et al., 2003; McAliley et al., 2006; Eaton et. al.,
752 2009; Hekkala et al., 2010; Hekkala et al., 2011; Meredith et al., 2011).

753 Using differing molecular techniques, it has been found that *C. niloticus*
754 consists of two separate paraphyletic taxa that can be divided into East African and
755 West African species (Hekkala et al., 2010; Hekkala et al., 2011; Meredith et al.,
756 2011; Oaks, 2011). Recent analysis of Egyptian mummified crocodiles by Hekkala et
757 al. (2011) found that they belong to the West African species, which supports
758 previous arguments that the two species lived in sympatry along the lower Nile
759 River. This provides strong support for referring the western clade back to the
760 species *Crocodylus suchus* Geoffroy Saint-Hilaire, 1807, as originally described.
761 Furthermore, Meredith et al. (2011) and Oaks (2011) found that the East African
762 clade of *C. niloticus* shares closer affinities with New World crocodylians than it does
763 with the western clade, providing strong evidence for trans-Atlantic dispersal of
764 *Crocodylus* from Africa. Considering the distance required for a trans-Atlantic
765 journey to reach the New World, the distance across the Mozambique Channel to
766 Madagascar (~450km) seems much less daunting.
767 In the study by Hekkala et al. (2010), populations of *C. niloticus* exhibited
768 genetic clustering that is consistent with Madagascar's isolation from Africa.
769 Interestingly, populations of *C. niloticus* sampled from northwestern Madagascar
770 exhibit weaker divergence from those from the Zambezi River drainage in
771 Zimbabwe than they do with other populations on the island (Hekkala et al., 2010).
772 This could represent a more recent colonization, suggesting that *C. niloticus*
773 dispersed to Madagascar through multiple dispersal events. Currently the timing of
774 *C. niloticus* first reaching the island is poorly known; our subfossil specimen (460 –
775 310 ybp) represents the first dated subfossil crocodylian described from

776 Madagascar, contributing a minimum date for arrival. Additionally, given its juvenile
777 status, we infer that there must have been an established breeding population of *C.*
778 *niloticus* on Madagascar by this date. As this specimen was discovered in the
779 northwest of the island, further research using molecular methods could possibly
780 determine if the specimen is consistent with results from Hekkala et al. (2010).
781 Another possibility, however unlikely, is that the specimen could belong to
782 *Crocodylus suchus*. Since it has been demonstrated that the two species lived
783 alongside each other in the lower Nile River (Hekkala et al., 2011), there is the
784 possibility that it could have dispersed to Madagascar as well. Although molecular
785 data is needed to test this hypothesis, there is currently no evidence that *C. suchus*
786 ever reached Madagascar.
787
788 **Conclusion**
789 The subfossil crocodile specimen collected from Anjohibe Cave is a
790 spectacularly preserved specimen and the only known juvenile crocodile
791 represented in the subfossil record of Madagascar. While both *C. niloticus* and *V.*
792 *robustus* have been documented from the cave (Goodman & Jungers, 2014), little
793 effort has been made to systematically describe and identify the fossils. Although
794 locally extinct from the cave, according to local residents *C. niloticus* was historically
795 present in the cave (personal communication to KES). Although nothing is known
796 about the growth and development of *V. robustus*, the skull of the subfossil specimen
797 possesses characters that strongly support its placement within *Crocodylus*, and
798 likely *C. niloticus*. Other than possible incipient squamosal horns that are evidently

present in older specimens, the evidence is very convincing that it is indeed not a juvenile *Voay robustus*. Because the only remaining crocodylian known from the Cenozoic of Madagascar is *Crocodylus niloticus*, it seems parsimonious to consider this specimen a juvenile *C. niloticus* until further evidence suggests otherwise.

Acknowledgements

We would like to thank the government of Madagascar for allowing us to conduct this research and the Department de Paléontologie et Anthropologie Biologique, Université d' Antananarivo, specifically A. Rasomiaramanana and H. Andriamialison for the opportunity to collaborate. Fieldwork was performed under a collaborative accord between Stony Brook University and the Université d' Antananarivo. Misaotra betsaka to the field team: Mark Loewen, Mike Getty, and to the Institute for the Conservation of Tropical Environments (ICTE/MICET) and B. Andriamihaja for logistical support in the field. We would like to thank Dr. Mark Goodwin and Dr. Pat Holroyd from the University of California Museum of Paleontology, Berkeley, California and Scott Williams from the Burpee Museum of Natural History in Rockford, Illinois for access to their collections. We would also like to thank Alan Resetar and the Field Museum of Natural History for access to their collections and for loaning of the *C. niloticus* specimen. Thank you to Dr. Christopher Vittore, MD and Radiologic technologist Dennis Esselman, RT(R) at Rockford Memorial Hospital for access to CT scanning and all of the post processing work they provided to make the data available and viewable. Special thanks to Patrick Price for the illustrations of the subfossil crocodile specimens, to Dr. Brooke

822 Crowley at the University of Cincinnati for the radiometric date on this specimen,
823 and Sarah Conway Romanelli for her preliminary work on this specimen.

824 **References**
825
826 Ali JR, Huber M. 2010. Mammalian biodiversity on Madagascar controlled by ocean
827 currents. Nature 463: 653-656.
828 Bailleul AM, Scannella JB, Horner JR, Evans, DC. 2013. Fusion patterns in the skull of
829 modern archosaurs reveal that sutures are ambiguous maturity indicators
830 for the Dinosauria. PLoS ONE 11(2): e0147687.
831 Bickelmann C. Klein N. 2009. The late Pleistocene horned crocodile *Voay robustus*
832 (Grandidier & Vaillant, 1872) from Madagascar in the Museum für
833 Naturkunde Berlin. Fossil Record 12 (1): 13-21.
834 Brochu CA. 1996. Closure of neurocentral sutures during crocodilian ontogeny:
835 implications for maturity assessment in fossil archosaurs. Journal of
836 Vertebrate Paleontology 16 (1): 49-62.
837 Brochu CA. 2000. Phylogenetic relationships and divergence timing of *Crocodylus*
838 based on morphology and the fossil record. Copeia 2000: 657-673.
839 Brochu CA. 2006. A new miniature horned crocodile from the Quaternary of Aldabra
840 Atoll, Western Indian Ocean. Copeia 2006: 149-158.
841 Brochu CA. 2007. Morphology, relationships, and biogeographical significance of an
842 extinct horned crocodile (Crocodylia, Crocodylidae) from the Quaternary of
843 Madagascar. Zoological Journal of the Linnean Society 150: 835-863.
844 Brochu CA, Njau J, Blumenschine RJ, Densmore LD. 2010. A new horned crocodile
845 from the Plio-Pleistocene hominid sites at Olduvai Gorge, Tanzania. PLoS
846 ONE 5(2): e9333.
847 Brook GA, Rafter MA, Railsback LB, Sheen S-W, Lundberg J. 1999. A high-resolution
848 proxy record of rainfall and ENSO since AD 1550 from layering in stalagmites
849 from Anjohibe Cave, Madagascar. The Holocene 9: 695-705.
850 Buckley GA. 2001. A skull of *Mahajangasuchus insignis* (Crocodyliformes) from the
851 Upper Cretaceous of Madagascar. Journal of Vertebrate Paleontology 21 (3)
852 supplement: A36
853 Buckley GA, Brochu CA. 1999. An enigmatic new crocodile from the Upper
854 Cretaceous of Madagascar. In D.M. Unwin (eds), Cretaceous Fossil
855 Vertebrates. Special Papers in Paleontology 60: 149–175.
856 Buckley GA, Brochu CA, Krause DW, Pol D. 2000. A pug-nosed crocodyliform from
857 the Late Cretaceous of Madagascar. Nature 405 (6789): 941-944.
858 Buffetaut E, Taquet P. 1979. Un nouveau crocodilien mesosuchien dans le
859 Campanien de Madagascar: *Trematochampsa oblita*, n. sp. Bulletin de la
860 Societe Geologique de France 2: 183–188.
861 Burney DA, James HF, Grady FV, Rafamantanantsoa J-G, Ramilisonina, Wright HT,
862 Cowart JB. 1997. Environmental change, extinction and human activity:
863 Evidence from caves in NW Madagascar. Journal of Biogeography 24: 755-
864 767.
865 Cope ED. 1861. List of the recent species of emydosaurian reptiles in the Museum of
866 the Acadamy of Natural Sciences. Proceedings of the Academy of Natural
867 Sciences of Philadelphia 12: 549–550.

868 Crowley BE, Samonds KE. 2013. Stable carbon isotope values confirm a recent
869 increase in grasslands in northwestern Madagascar. The Holocene 23 (7):
870 1066-1073.
871 Cuvier G. 1807. Sur les differentes especes de crocodiles vivants, et sur leurs
872 caracteres distinctifs. Annales du Museum d'Histoire Naturelle 10: 8–66.
873 Daudin FM. 1802. Histoire naturelle generale et particuliere des reptile. Volume 2.
874 Dufart, Paris.
875 Eaton MJ, Martin A, Thorbjarnarson J, Amato G. 2009. Species-level diversification of
876 African dwarf crocodiles (genus *Osteolaemus*): a geographical and
877 phylogenetic perspective. Molecular Phylogenetics and Evolution 50: 496-
878 506.
879 Faure M, Guérin C, Genty D, Gommery D, Ramanivosoa B. 2010. Le plus ancien
880 hippopotame fossile (*Hippopotamus laloumena*) de Madagascar (Belobaka,
881 Province de Mahajanga). Comptes Rendus Palevol, 9 (4): 155-162.
882 Fauvel AA. 1879. Alligators in China: Their history, description, and identification. J.
883 North-China Branch Royal Asiatic Society (Shanghai), N.S. 13: 1–36.
884 Geoffroy Saint-Hilaire E. 1807. Description de deux crocodiles qui existent dans le
885 Nil, compares au crocodile de Saint-Domingue. Annales du Museum
886 d'Histoire Naturelle 10: 67–86, 264 + 2 pl.
887 Godfrey LR, Jungers WL, Simons EL, Chatrath PS. Rakotosamimanana B. 1999. Past
888 and present distributions of lemurs in Madagascar. In Rakotosamimanana, B.,
889 Rasamimanana, H., Ganzhorn, J. and Goodman, S. (eds.) New Directions in
890 Lemur Studies (pp. 19-53). Springer US.
891 Goodman SM, Jungers WL. 2014. Extinct Madagascar: Picturing the Island's Past.
892 University of Chicago Press, Chicago, 296 pp.
893 Grandidier A, Vaillant L. 1872. Sur le crocodile fossile d'Amboulintsatre
894 (Madagascar). Comptes Rendus de l'Academie des Sciences de Paris 75: 150–
895 151.
896 Griggs G, Kirshner D. 2015. Biology and Evolution of Crocodylians. CSIRO Publishing,
897 Ithaca and London, 649 pp.
898 Hekkala ER, Amato G, DeSalle R. Blum MJ. 2010. Molecular assessment of population
899 differentiation and individual assignment potential of Nile crocodile
900 (*Crocodylus niloticus*) populations. Conservation Genetics 11: 1435-1443.
901 Hekkala E, Shirley MH, Amato G, Austin JD, Charters S, Thorbjarnarson J, Vliet KA,
902 Houck ML, DeSalle R, Blum MJ. 2011. An ancient icon reveals new mysteries:
903 mummy DNA resurrects a cryptic species within the Nile crocodile. Molecular
904 Ecology 20: 4199-4215.
905 Irmis RB, Nesbitt SJ, Sues H-D. 2013. Early Crocodylomorpha. Geological Society of
906 London Special Publication 379: 275-302.
907 Ikejiri T. 2012. Histology-based morphology of the neurocentral synchondrosis in
908 *Alligator mississippiensis* (Archosauria, Crocodylia). The Anatomical Record
909 295: 18-31.
910 Ikejiri T. 2015. Modes of ontogentic allometric shifts in crocodylian vertebrae.
911 Biological Journal of the Linnean Society 116: 649-670.
912

913 Krause DW, O'Connor PM, Rogers KC, Sampson SD, Buckley GA, Rogers RR. 2006.
914 Late Cretaceous terrestrial vertebrates from Madagascar: Implications for
915 Latin American biogeography. Annals of the Missouri Botanical Garden 93
916 (2): 178-20.
917 Latham J. 1790. Index ornithologicus, sive systema ornithologiae: Complectens
918 avium divisionem in classes, Ordines, Genera, Species, Ipsarumque
919 Varietates. Volume 2. Leigh and Sotheby, London, 665 pp.
920 Laurenti JN. 1768. Specimen Medicum, Exhibens Synopsis Reptilium Emendatum
921 cum Experimentalis Circa Venena et Antidota Reptilium Austriacorum.
922 Joannis Thomae nobilis de Trattern, Vienna, 214 pp.
923 Longrich NR, Field DJ. 2012. *Torosaurus* is not *Triceratops*: Ontogeny in
924 chasmosaurine ceratopsids as a case study in dinosaur taxonomy. PLoS ONE
925 7(2): e32623
926 MacPhee RD. 1994. Morphology, adaptations, and relationships of *Plesiorycteropus*,
927 and a diagnosis of a new order of eutherian mammals. Bulletin of the
928 American Museum of Natural History no. 220: 1-214.
929 McAliley L, Willis R, Ray D, White P, Brochu C, Densmore L. 2006. Are crocodiles
930 really monophyletic?-Evidence for subdivisions from sequence and
931 morphological data. Molecular Phylogenetics and Evolution 39: 16-32.
932 Meredith RW, Hekkala ER, Amato G, Gatesy J. 2011. A phylogenetic hypothesis for
933 *Crocodylus* (Crocodylia) based on mitochondrial DNA: Evidence for a trans-
934 Atlantic voyage from Africa to the New World. Molecular Phylogenetics and
935 Evolution 60: 183-191.
936 Mook CC. 1921a. Individual and age variations in the skulls of recent Crocodilia.
937 Bulletin of the American Museum of Natural History no. 44: 51-73.
938 Mook CC. 1921b. Skull characters of recent Crocodilia with notes on the affinities of
939 the recent genera. Bulletin of the American Museum of Natural History no.
940 44: 123-268.
941 Muldoon KM, Cowley BE, Godfrey LR, Rasoamiaramanana A, Aronson A, Jernvall J,
942 Wright PC, Simons EL. 2012. Early Holocene fauna from a new subfossil site:
943 A first assessment from Christmas River, south central Madagascar.
944 Madagascar Conservation & Development 7 (1): 23-29.
945 Myers N, Mittermeier RA, da Fonseca GAB, Kent J. 2000. Biodiversity hotspots for
946 conservation priorities. Nature 403: 853-858.
947 Newton RB. 1893. On the discovery of a secondary reptile in Madagascar:
948 *Steneosaurus baroni* (n. sp.); with a reference to some Post-Tertiary
949 vertebrate remains from the same country recently acquired by the British
950 Museum (Natural History). Geological Magazine (Decade III) 10 (05): 193–
951 198.
952 Oaks JR. 2011. A time-calibrated species tree of Crocodylia reveals a recent radiation
953 of the true crocodiles. Evolution 66 (11): 3285-3297.
954 O'Connor PM, Sertich JW, Stevens NJ, Roberts EM, Gottfried MD, Hieronymus TL,
955 Jinnah ZA, Ridgely R, Ngasala SE, Temba J. 2010. The evolution of mammal-
956 like crocodyliforms in the Cretaceous period of Gondwana. Nature 466: 748-
957 751.

Rasmusson-Simons EL, Buckley GA. 2009. New Material of "*Trematochampsa" oblita* (Crocodyliformes,Trematochampsidae) from the Late Cretaceous of Madagascar. Journal of Vertebrate Paleontology 29 (2): 599–604.

Rosenberger AL, Godfrey LR, Muldoon KM, Gunnell GF, Andriamialison H, Ranivoharimanana L, Ranaivoarisoa JF, Rasoamiaramanana AH, Randrianasy J, Amador FE. 2015. Giant subfossil lemur graveyard discovered, submerged, in Madagascar. Journal of Human Evolution 81: 83-87.

Samonds KE. 2007. Late Pleistocene bat fossils from Anjohibe Cave, northwestern Madagascar. Acta Chiropterologica 9 (1): 39-65.

Samonds KE, Godfrey LR, Ali JR, Goodman SM, Vences M, Sutherland MR, Irwin MT, Krause DW. 2012. Spatial and temporal arrival patterns of Madagascar's vertebrate fauna explained by distance, ocean currents, and ancestor type. Proceedings of the National Academy of Sciences (USA) 109: 5352-5357.

Samonds KE, Godfrey LR, Ali JR, Goodman SM, Vences M, Sutherland MR, Irwin MT, Krause DW. 2013. Imperfect isolation: factors and filters shaping Madagascar's extant vertebrate fauna. PLoS ONE 8(4): e62086.

Sampson SD, Ryan MJ, Tanke DH. 1997. Craniofacial ontogeny in centrosaurine dinosaurs (Ornithischia: Ceratopsidae): taxonomic and behavioral implications. Zoological Journal of the Linnean Society 121: 293-337.

Schmitz A, Mansfeld P, Hekkala E, Shine T, Nickel H, Amato G, Bohme W. 2003. Molecular evidence for species level divergence in African Nile Crocodiles *Crocodylus niloticus* (Laurenti, 1786). Comptes Rendus Palevol 2: 703-712.

Schneider JG. 1801. Historiae Amphibiorum Naturalis et Literariae. Fascciculus Secundus Continenes Crocodilos, Scincos, Chamaesauras, Boas. Pseudoboas, Elapes, Angues. Amphisbaenas et Caecilias. Frommani, Jena, 364 pp.

Storey M, Mahoney JJ, Saunders AD, Duncan RA, Kelley SP, Coffin MF. 1995. Timing of hot spot-related volcanism and the breakup of Madagascar and India. Science 267 (5199): 852-855.

Turner AH, Sertich JW. 2010. Phylogenetic history of *Simosuchus clarki* (Crocodyliformes: Notosuchia) from the Late Cretaceous of Madagascar. Journal of Vertebrate Paleontology 30 (6, Supplement): 177-236.

Turner AH. 2006. Osteology and phylogeny of a new species of *Araripesuchus* (Crocodyliformes: Mesoeucrocodylia) from the Late Cretaceous of Madagascar. Historical Biology 18 (3): 255-369.

Witmer LM. 1995. Homology of facial structures in extant archosaurs (birds and crocodilians), with special reference to paranasal pneumaticity and nasal conchae. Journal of Morphology 225: 269-327.

Zanno LE, Drymala S, Nesbitt SJ, Schneider VP. 2015. Early crocodylomorph increases top tier predator diversity during rise of dinosaurs. Scientific Reports 5. Article number 927.

998 **Figure Captions**
999
1000 **Figure 1.** Locality Map. Map showing location of the Anjohibe Cave system in
1001 Northwest Madagascar. Scale is in km. (Adapted from Samonds, 2007).

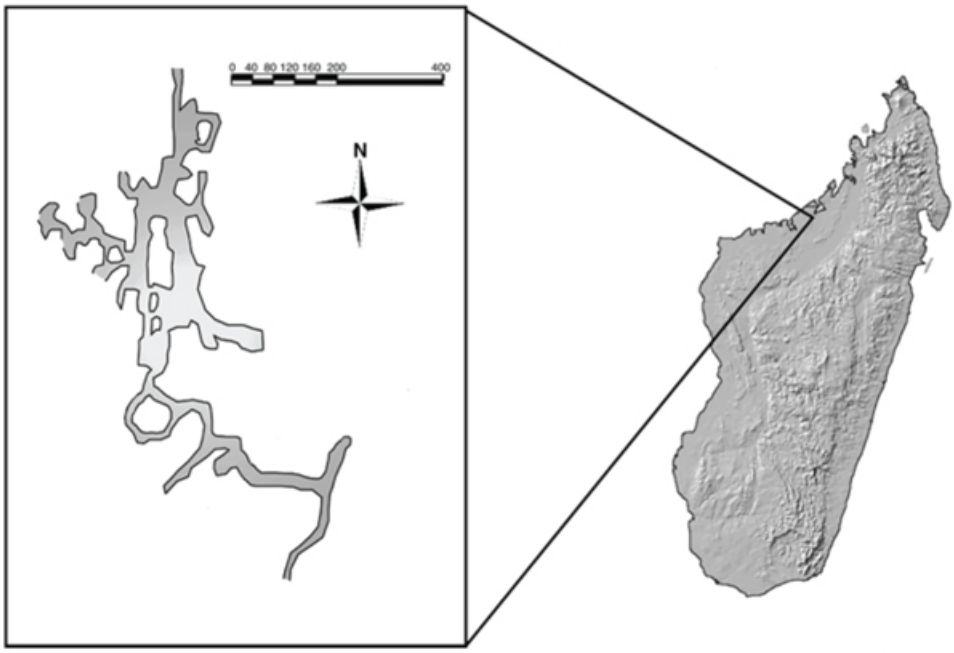

1002
1003

Figure 2. UAP-03.791, crocodylian specimen recovered from Anjohibe Cave, Northwestern Madagascar. Scale bar = 10 cm.

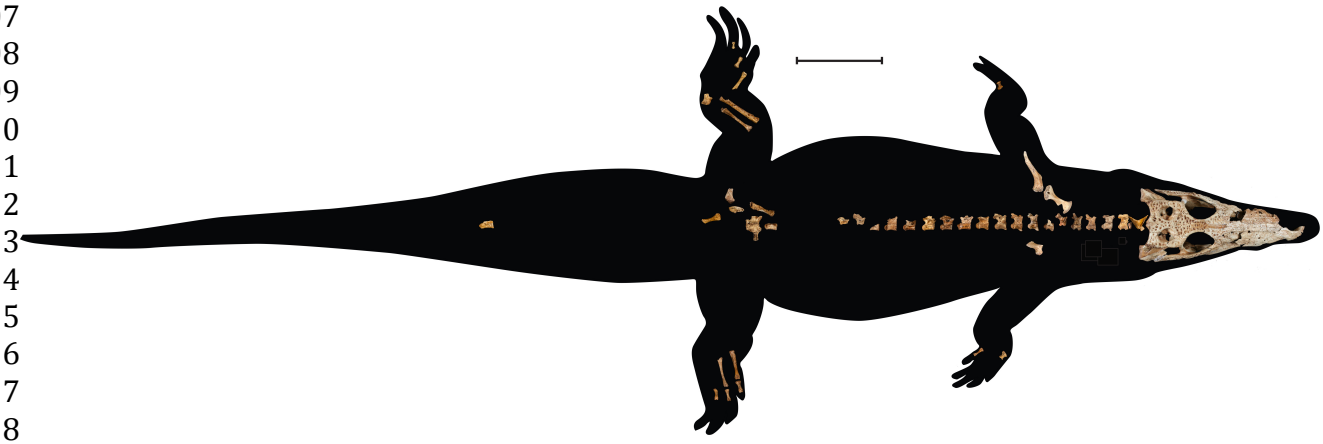

Figure 3. Skull of UAP-03.791 in A, dorsal view; B, right lateral view;. C, ventral view; D. Occipital View. Top scale bar = 10 cm; Bottom scale bar = 5 cm. Abbreviations : bo, basioccipital; ect, ectopterygoid; eo, exoccipital; eoa, external otic aperture; f, frontal; fm, foramen magnum; ic, internal choana; j, jugal; lac, lacrimal; lcf, lateral carotid foramen; mx, maxilla; m5, maxillary alveolus 5; ns, nasal; oc, occipital condyle; orb, orbit; pa, parietal; pmx, premaxilla; pm 4, premaxillary alveolus 4; po, postorbital; prf, prefrontal; pt, pterygoid; q, quadrate; qj, quadratojugal; s.mx, sutural surface on palatine for maxilla; soc, supraoccipital; sq, squamosal; vf, vagus foramen.

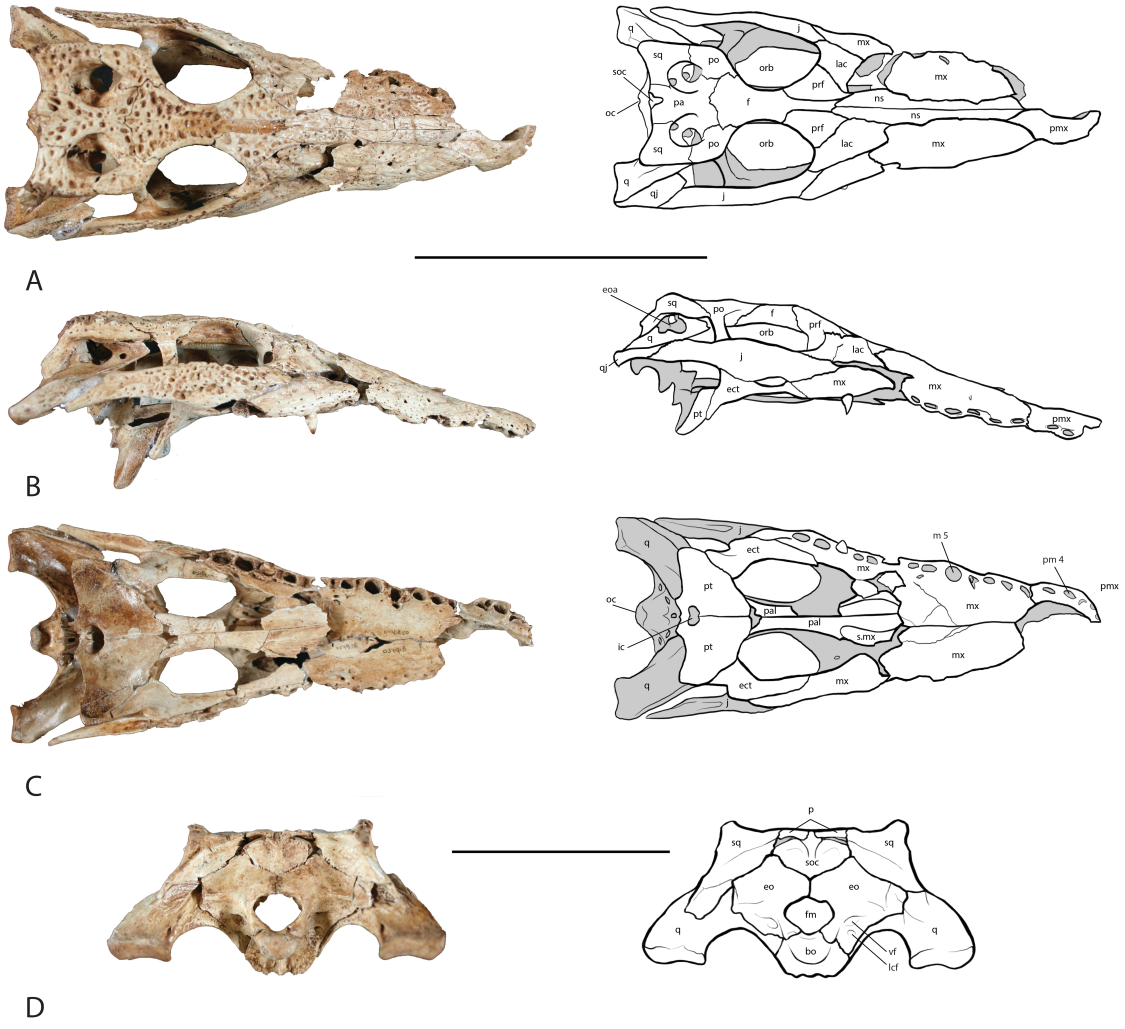

Figure 4. Postcranial remains of UAP-03.791. A, Partial left humerus, dorsal view; B, Left coracoid, dorsal view; C, partial right scapula, ventral view; D, left radiale, dorsal view; E, right radiale, dorsal view; F, metacarpal, dorsal view; G, partial left ilium, lateral view; H, partial left ischium, medial view; I, partial left pubis, medial view; J, partial left tibia, dorsal view; K, partial left fibula, dorsal view; L, left calcaneum, lateral view; M-O, left metatarsals. Scale = 5 cm

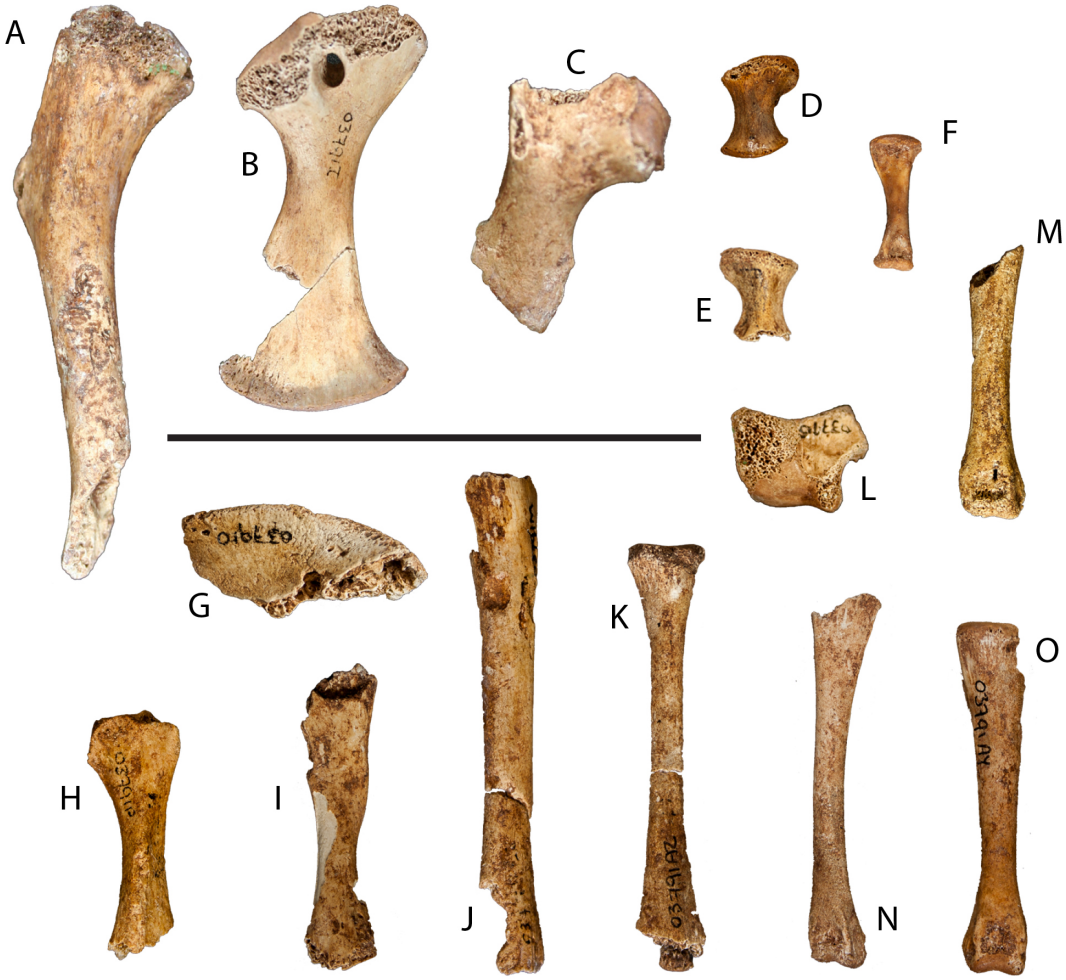

Figure 5. Right maxilla. Medial view of the right maxilla showing the wall of the caviconchal recess. A, UAP-03.791 Anjohibe Cave specimen. B, uncatalogued UA specimen, *Voay robustus*. Abbreviations: ccr, medial wall of the caviconchal recess; cr, caecal recesses on the wall of the caviconchal recess; s.n, sutural surface with the nasal; s.pmx, sutural surface with the premaxilla. Scale = 1 cm.

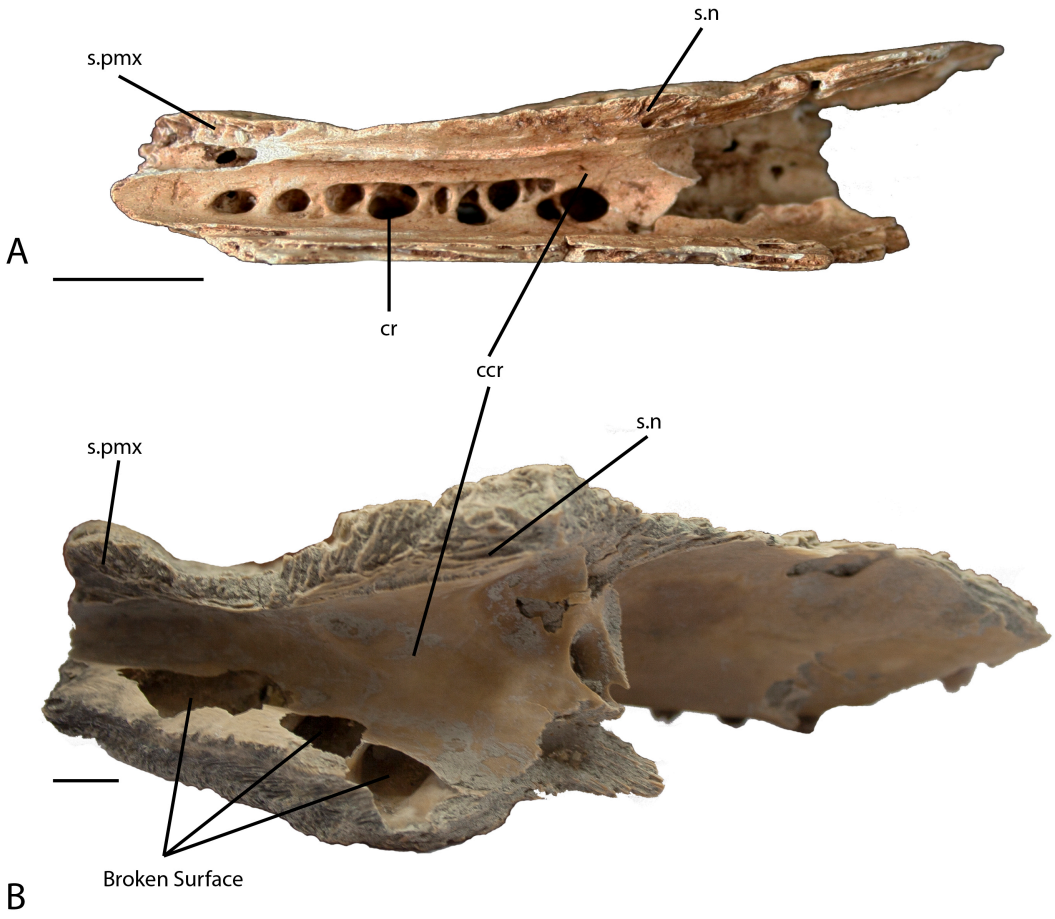

Figure 6. Mandible of UAP-03.791. Top, dorsal view; bottom, right lateral view. Abbreviations: d4, alveolus for dentary tooth number 4; emf, external mandibular fenestra; faa, articular foramen aereum; gf, glenoid fossa of articular. Scale = 10 cm

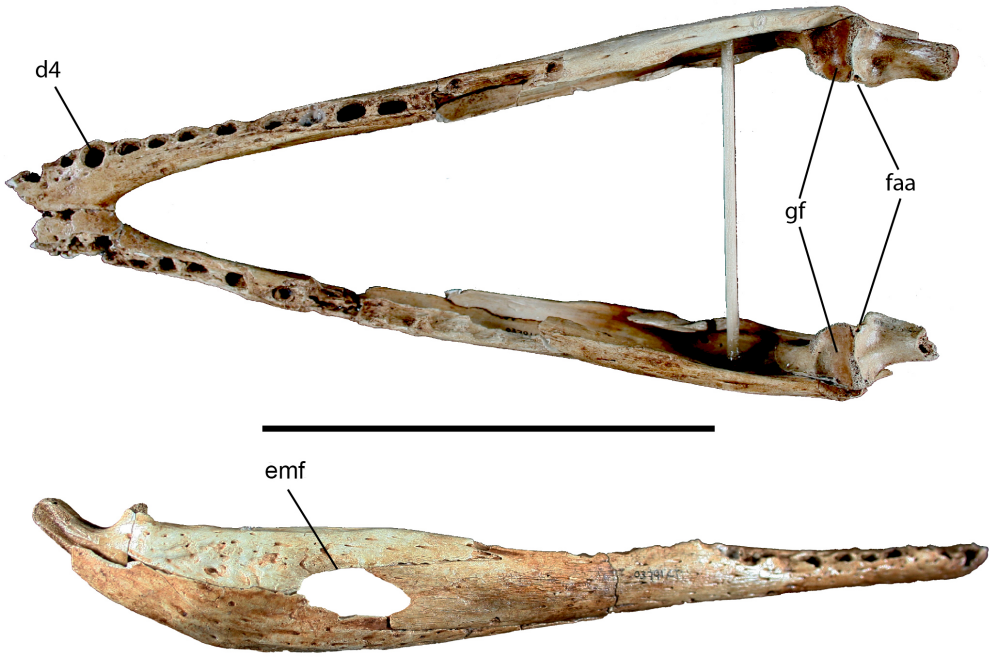

Figure 7. Teeth found in association with UAP-03.791. A, anterior tooth in (l-r) lingual view, labial view, and lateral view; B, posterior tooth in (l-r) lingual view and labial view. Abbreviations: ca, carinae; str, striations. Scale = 1 cm

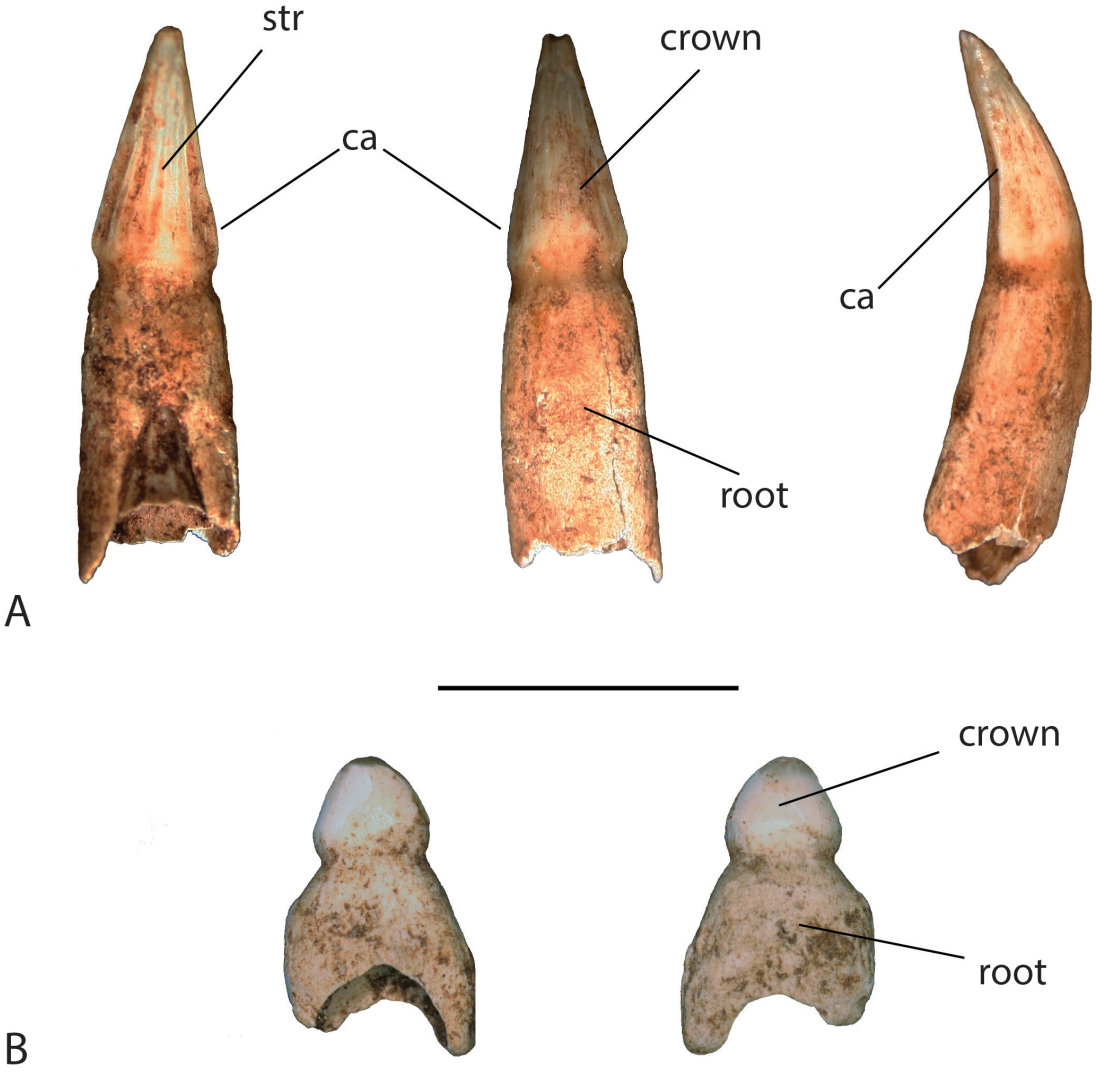

Figure 8. Neurocentral suture closure. Elements of the vertebral column showing degree of disarticulation and neurocentral suture closure. A, atlas elements; B, axis; C, cervical vertebra 6; D, posterior thoracic vertebra; E, anterior thoracic vertebra; F, first sacral vertebra. Abbreviations: hyp, hypapophysis; ic, intercentrum; na, neural arch; ns, neurocentral suture; od, odontoid process; pro, proatlas. Scale = 1 cm

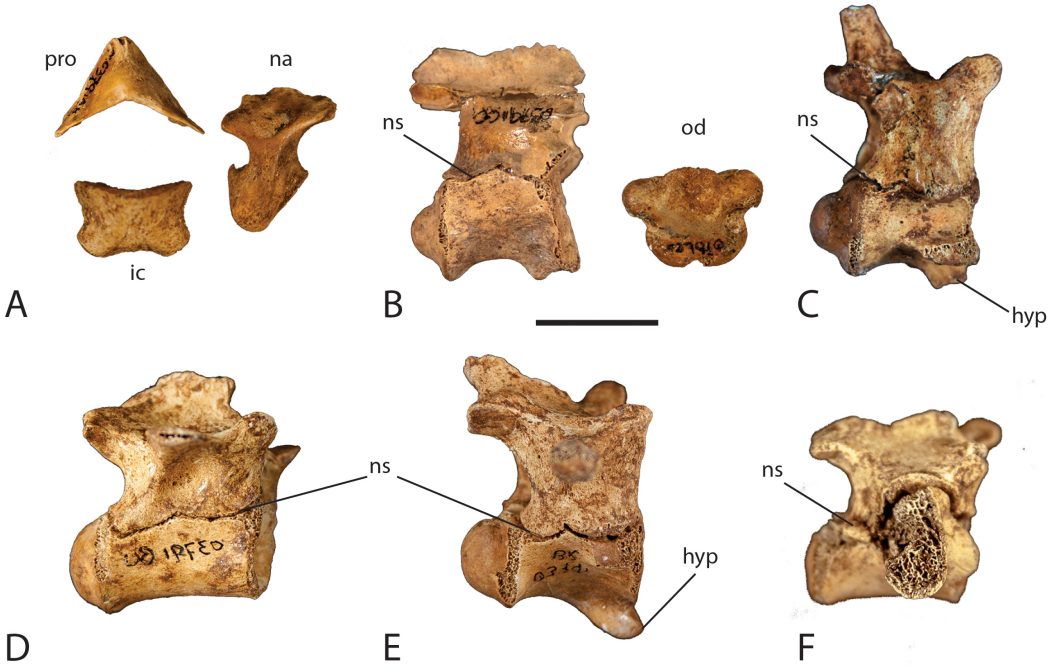

Figure 9. Skull shape comparison. Dorsal view. A, FMNH 37216, *Crocodylus niloticus*. B, UAP-03.791, Anjohibe Cave specimen. C, UCMP 140796, *C. niloticus*. Scale = 5 cm.

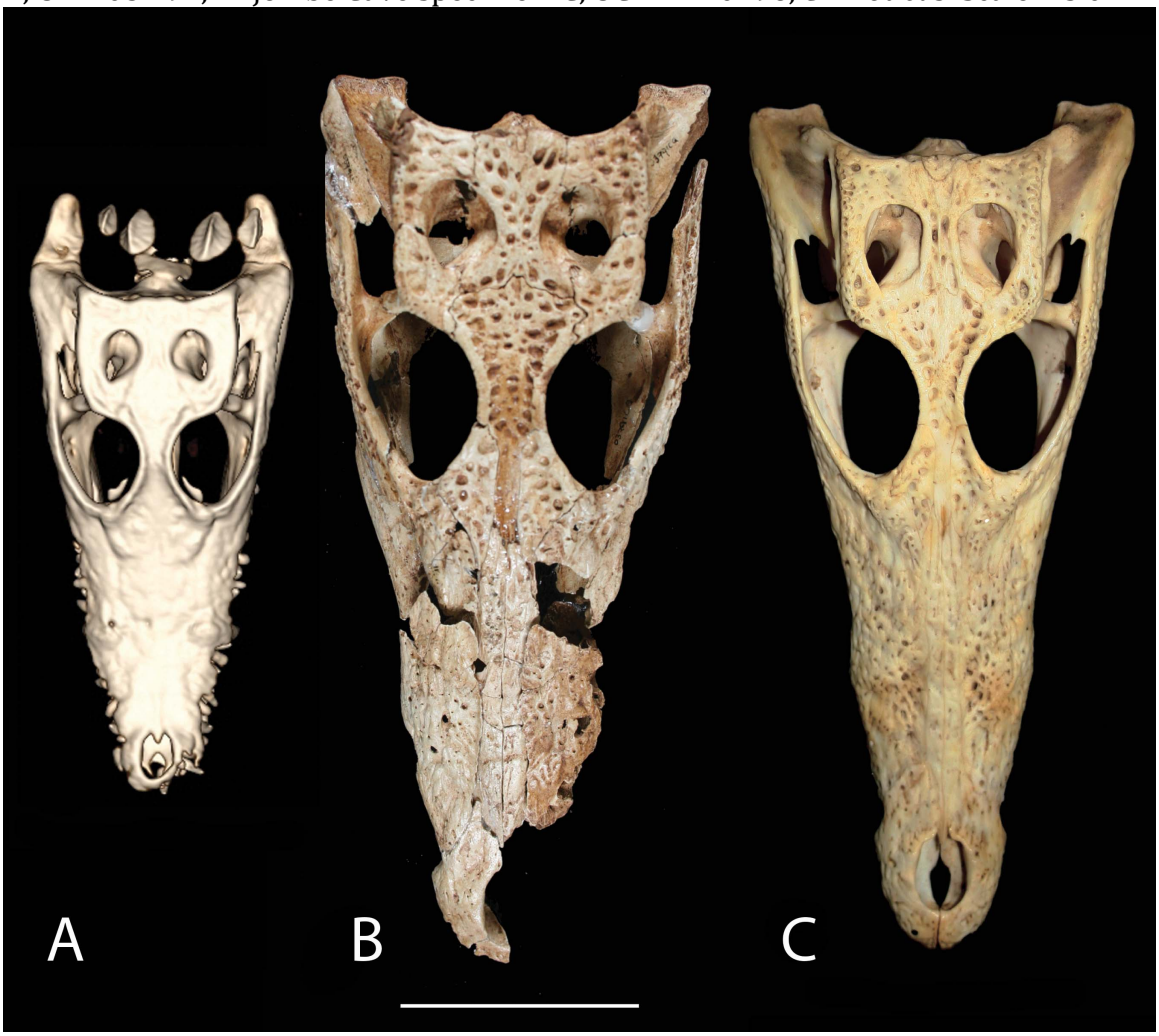

Figure 10. Ventral view of the internal choana of *Crocodylus niloticus* and *Voay robustus*. A, uncatalogued UA specimen, *Voay robustus* (left) and uncatalogued UA specimen, *Crocodylus niloticus* (right), Scale = 2 cm. B. Subfossil specimen UAP-03.791, Scale = 10 cm; C, computed tomography image of *Crocodylus niloticus,* FMNH 37216, Scale = 5 cm. Abbreviations: cn, choanal neck; ic, internal choana; oc, occipital condyle.

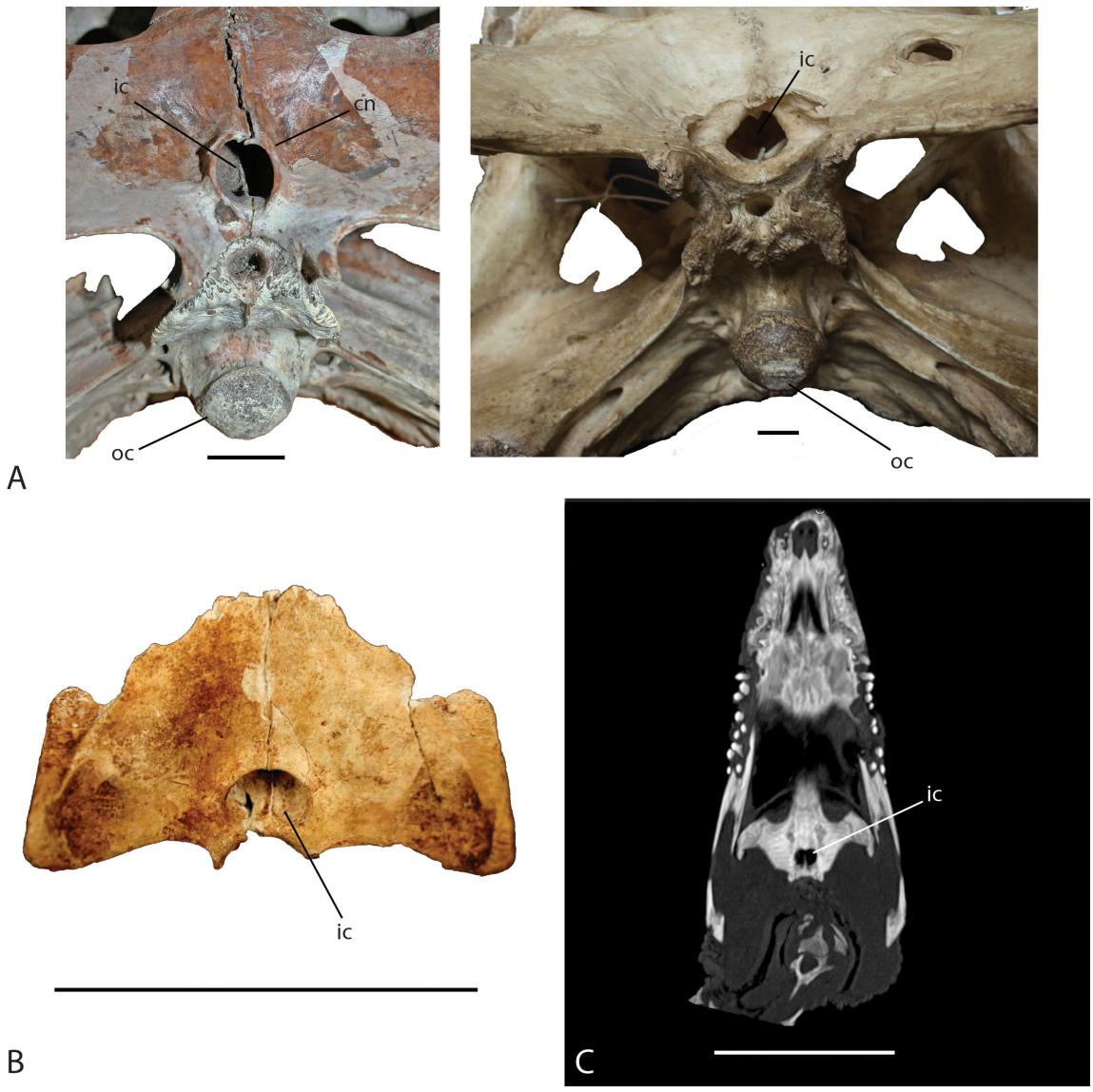

Figure 11. Squamosal horns. Left lateral view and posterior view of skulls showing degree of squamosal horn development. A, uncatalogued UA specimen, *Crocodylus niloticus*. B, uncatalogued UA specimen, *Voay robustus*. Skulls have been scaled to the same size for comparison. Abbreviation: sh, squamosal horn. Scale = 10 cm.

Figure 12. Posterior view of skulls showing degree of squamosal horn development in young individuals. A, UAP-03.791, Anjohibe Cave specimen. B, FMNH 37216, *Crocodylus niloticus*. Abbreviation: sh, squamosal horns. Scale = 5 cm.